Landes Bioscience www.landesbioscience.com

Supplemental Material to:

Axelle Loriot, Aurélie Van Tongelen, Jordi Blanco, Simon Klaessens, Julie Cannuyer, Nicolas van Baren, Anabelle Decottignies, Charles De Smet

A novel cancer-germline transcript carrying pro-metastatic miR-105 and TET-targeting miR-767 induced by DNA hypomethylation in tumors

Epigenetics 2014; 9(8)
http://dx.doi.org/10.4161/epi.29628
http://www.landesbioscience.com/journals/epigenetics/article/29628/

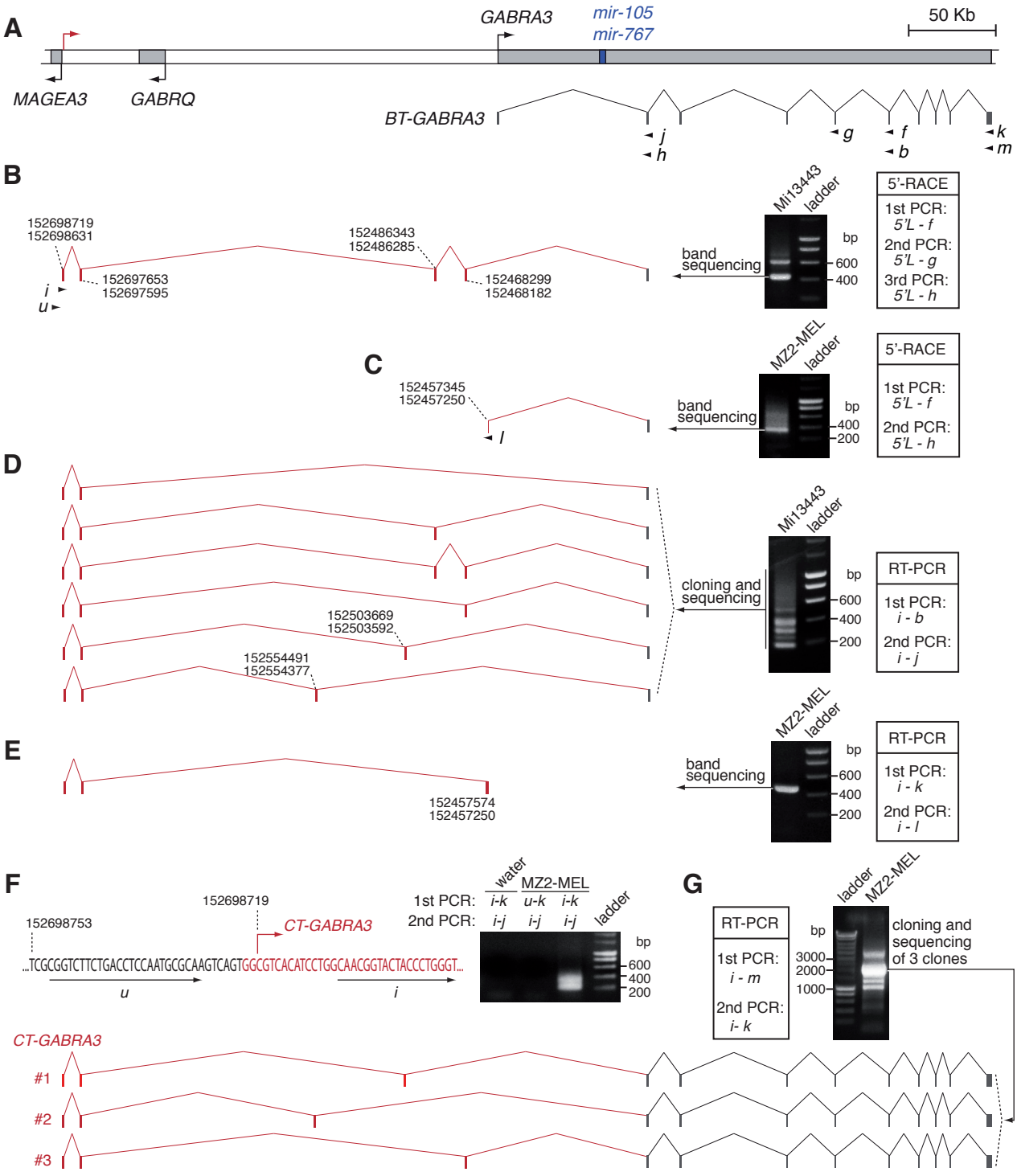

Figure S1. Characterization of the novel *CT-GABRA3* transcript by 5'-RACE and RT-PCR experiments.
(A) Schematic representation of the *GABRA3* locus, with the exon/intron structure of the reference *GABRA3* gene (XM_005274659.1, NCBI RefSeq), which we re-named *BT-GABRA3*. Arrowheads indicate the approximate position and orientation of PCR primers used in subsequent experiments. **(B)** A first 5'-RACE experiment, using the SMART technology, was performed on total RNA extracted from the Mi13443-MEL melanoma cell line. Three rounds of nested PCR were applied, using the 5'L adapter sense primer and different antisense primers, as indicated. PCR products resulting from the third amplification round were submitted to gel electrophoresis, and the indicated band was extracted and sequenced. Exon/intron structure of the corresponding transcript is shown, and positions of exons relative to the reference GRCh38 human genome assembly are given. Of note, the upper band was found to result from non-specific amplification. **(C)** A second 5'-RACE experiment, with two rounds of nested PCR, was applied to melanoma cell line MZ2-MEL, and led to the identification of an alternative, likely truncated (see panel E), transcript variant. **(D)** Total RNA from Mi13443-MEL was reverse-transcribed, and submitted to two nested PCR with the indicated primers. Gel analysis revealed amplification of several bands. The bulk PCR product was cloned into a vector, and individual clones were sequenced. This led to the characterization of several splicing variants. **(E)** Inclusion of the exon identified by 5'-RACE in MZ2-MEL (see panel C) in *CT-GABRA3* transcripts also containing upstream exons was verified by an RT-PCR experiment using corresponding primers, as indicated. **(F)** Initiation of *CT-GABRA3* transcription at the position defined by 5'-RACE experiments was corroborated by the lack of RT-PCR signal when a PCR primer (u) located just upstream of that position was used. **(G)** A final experiment, combining RT-PCR, bulk cloning, and individual clone sequencing, was performed to verify that *CT-GABRA3* transcripts comprise newly indentified upstream exons linked to all exons but exon 1 of the referenced *BT-GABRA3* gene.

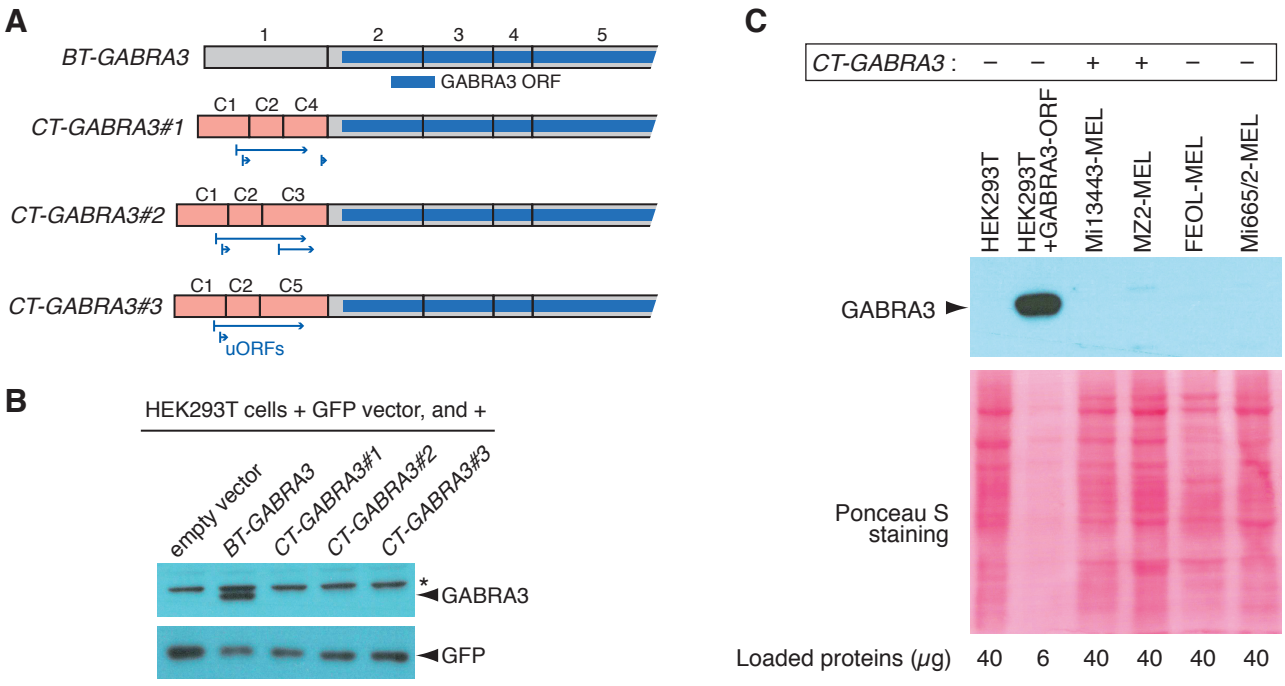

Figure S2. Short upstream open reading frames (uORFs) in *CT-GABRA3* mRNAs inhibit translation of the GABRA3 protein.

(A) Expression vectors were constructed, which contained the full length ORF of *GABRA3* preceded by the 5' UTR of either *BT-GABRA3* or three splice variants of *CT-GABRA3* (#1 to #3; see Fig. E2G). Blue arrows below *CT-GABRA3* transcripts delineate uORFs. Of note, two of these originate in the most 5' exon (C1), which is generally present in all *CT-GABRA3* splice variants. **(B)** These expression vectors, as well as an empty control vector, were transfected together with a GFP-expressing vector into HEK293T cells. Proteins were extracted from transfected cells and analyzed by Western blotting for the presence of the GABRA3 protein (anti-GABRA3; #ab23334, Abcam). Immunodetection of GFP (anti-GFP; #ab290, Abcam) served to verify similar transfection efficiencies. The results revealed marked inhibition of GABRA3 translation in *CT-GABRA3* transcripts. * non-specific band. **(C)** The presence of the GABRA3 protein was examined in melanoma cell lines that do (+) or do not (-) express *CT-GABRA3*. None of these cell lines expressed *BT-GABRA3*. HEK293T cells that had been transfected with an expression vector carrying the GABRA3 ORF were used as positive control. Loaded protein amounts are indicated, and were verified after Ponceau S staining. The results show that the GABRA3 protein remains undected in *CT-GABRA3*-expressing cell lines.

melanoma tissues (n=24)		
	GABRA3 +	*GABRA3* –
MAGEA3 +	17	1
MAGEA3 –	0	7

$p = 1.66 \times 10^{-5}$ (Fisher exact test)

NSCLC tissues (n=24)		
	GABRA3 +	*GABRA3* –
MAGEA3 +	11	8
MAGEA3 –	0	8

$p = 5.80 \times 10^{-3}$ (Fisher exact test)

Figure S3. *GABRA3* and *MAGEA3* show frequent co-activation in melanoma and non-small cell lung carcinoma (NSCLC) tissue samples.

Tumor samples were analyzed by RT-PCR for the expression of *GABRA3* and *MAGEA3*. For each tumor type, the number of samples that scored either positive or negative for one or both genes was reported in a 2X2 contingency table. Significant tendency of co-expression of the two genes was validated by a Fisher exact test.

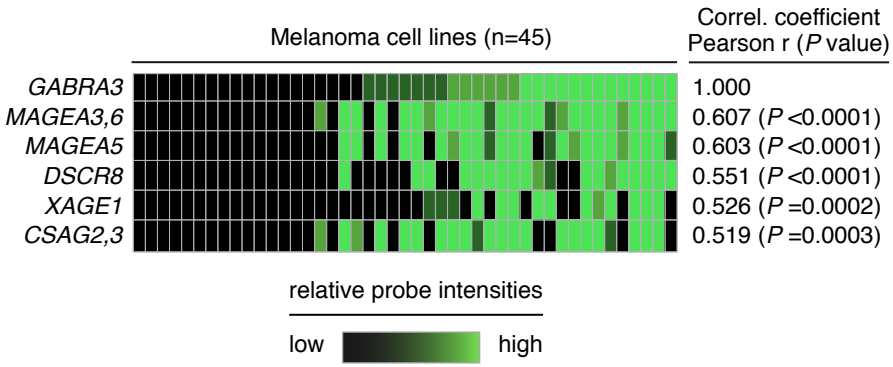

Figure S4. Activation of *GABRA3* transcripts in melanoma cell cultures correlates with that of CG genes.

Publicly available gene expression microarray data obtained from 45 melanoma cell cultures (dataset GSE4843) were downloaded. Relative probe intensities are reported by the indicated color code in the grid, with each column corresponding to a melanoma cell culture, and each row to a gene. Melanoma cell cultures were ordered according to *GABRA3* relative probe intensity values. Probe intensities for several known CG genes are also depicted (*MAGEA3* and *MAGEA6*, as well as *CSAG2* and *CSAG3* cannot be distinguished because of high sequence identity). Correlation coefficients between relative probe intensity values of CG genes and *GABRA3* were calculated. These revealed a significant trend of co-activation of *GABRA3* with CG genes.

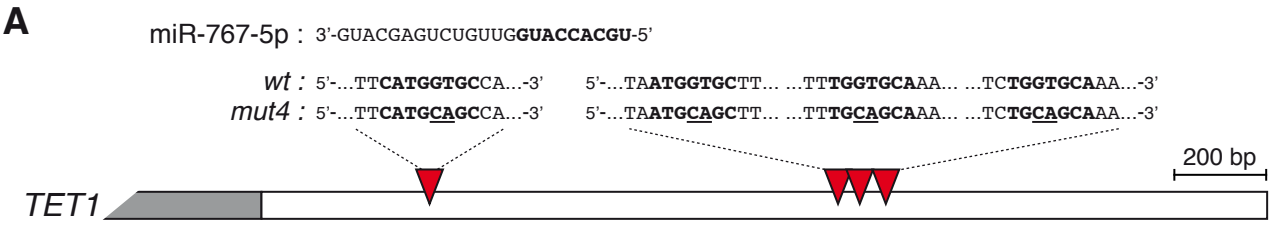

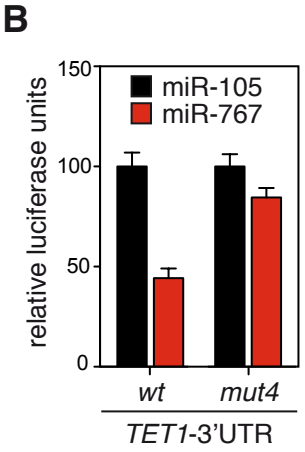

Figure S5. *TET1* regulation by miR-767 is impaired by mutations in 3'-UTR target sequences.

(A) Schematic representation of the 3'-UTR of *TET1* (empty bar) with the location of miR-767 seed sequences indicated by red triangles (only 7-mer and 8-mer seeds are depicted). The sequence of miR-767(-5p) is given, as well as the seed match sequences in the 3'-UTR of *TET1* (wt). A mutant form of the 3'UTR of *TET1* was generated (mut4), which contains the indicated nucleotide changes (underligned) in each of the four seed sequences. **(B)** HEK293T cells were co-transfected with a luciferase reporter gene linked to either the wt or the mut4 *TET1* 3'-UTR, and with the indicated miRNAs. Renilla luciferase were measured 24h after transfection, and were normalized with respect to the Firefly luciferase reporter carried on the same vector. Luciferase units are expressed relative to miR-105-transfected control cells, and represent means ±SD (n=4).

Table S1. Description of human tumor tissue samples

Melanoma tissue samples				
Ref	Patient code	Sex*	Age**	type of lesion
#1	LB1616	F	77	cutaneous melanoma, breast metastasis
#2	LG37	F	36	cutaneous melanoma, iliac node metastasis
#3	EN7	F	35	cutaneous melanoma, leg metastasis
#4	CP30	F	n/a	cutaneous melanoma, lymph node metastasis
#5	LB2077	F	28	metastatic cutaneous melanoma
#6	DDHK0002	M	56	metastatic cutaneous melanoma
#7	DDHK0002	M	56	cutaneous melanoma, leg in transit metastasis
#8	KUL73	F	71	cutaneous melanoma, satellite nodule
#9	LB2201	F	45	cutaneous melanoma, epithrochlear lymph node metastasis
#10	CP64	M	82	cutaneous melanoma, clavicular subcutaneous nodule
#11	KUL73	F	71	metastatic cutaneous melanoma
#12	VUB39	F	73	cutaneous melanoma, axillary node metastasis
#13	BB132	M	70	cutaneous melanoma, thoracic subcutaneous nodule
#14	LB168	M	53	cutaneous melanoma, mesenteric lymph node metastasis
#15	KUL73	F	71	cutaneous melanoma, inflammatory cutaneous nodule
#16	LB2077	F	28	cutaneous melanoma, intracardiac metastasis
#17	EB81	F	70	cutaneous melanoma, lymph node metastasis
#18	LB2269	M	62	cutaneous melanoma, axillary lymph node metastasis
#19	LB2259	F	74	cutaneous melanoma, thoracic subcutaneous nodule
#20	LB2370	M	39	cutaneous melanoma, inguinal lymph node metastasis
#21	LB2293	F	53	cutaneous melanoma, lymph node metastasis
#22	LB2357	M	62	cutaneous melanoma, supraclavicular lymph node metastasis
#23	CP67	F	44	cutaneous melanoma, left axillary lymphadenopathy
#24	LB2174	F	49	cutaneous melanoma, subcutaneous nodule
#25	LB2439	F	33	cutaneous melanoma, mediastinal lymph node metastasis
#26	DDHK0062	M	42	cutaneous melanoma, leg in transit metastasis
#27	LB2174	F	49	cutaneous melanoma, subcutaneous nodule
#28	LB2652	M	n/a	cutaneous melanoma, temporal lobe metastasis
#29	LB1572	M	36	benign nevus

Non-small cell lung carcinoma tissus samples				
Ref	Patient code	Sex	Age	type of lesion
#1	LB1214	M	65	epidermoid carcinoma, primary tumor
#2	LB498	M	55	epidermoid carcinoma, calf muscle metastasis
#3	LB973	M	62	epidermoid carcinoma, primary tumor
#4	LB1005	M	68	epidermoid carcinoma, primary tumor
#5	LB1006	F	67	epidermoid carcinoma, primary tumor
#6	LB1007	n/a	60	epidermoid carcinoma, primary tumor
#7	LB498	M	55	epidermoid carcinoma, recurrent calf muscle metastasis
#8	LB1061	M	62	epidermoid carcinoma, primary tumor
#9	LB1080	M	68	epidermoid carcinoma, primary tumor
#10	LB1102	M	49	epidermoid carcinoma, primary tumor
#11	LB1104	M	77	epidermoid carcinoma, primary tumor
#12	LB1123	M	n/a	epidermoid carcinoma, primary tumor
#13	LB1124	M	n/a	epidermoid carcinoma, primary tumor
#14	LB1125	M	66	epidermoid carcinoma, primary tumor
#15	LB1135	M	74	epidermoid carcinoma, primary tumor
#16	LB1136	F	68	epidermoid carcinoma, primary tumor
#17	LB1152	M	64	epidermoid carcinoma, primary tumor
#18	LB1156	M	54	epidermoid carcinoma, primary tumor
#19	LB911	M	73	epidermoid carcinoma, primary tumor
#20	LB1201	M	72	epidermoid carcinoma, primary tumor
#21	LB1211	M	72	epidermoid carcinoma, primary tumor
#22	LB1210	M	63	epidermoid carcinoma, primary tumor
#23	LB1222	M	69	epidermoid carcinoma, primary tumor
#24	LB1229	M	73	epidermoid carcinoma, primary tumor
#25	LB1239	M	64	epidermoid carcinoma, primary tumor
#26	LB1261	M	74	epidermoid carcinoma, primary tumor
#27	LB1303	M	n/a	epidermoid carcinoma, primary tumor

* M = male; F = female
** Age at tissue sample resection

Table S2. Oligonucleotidic primers and probe sequences

Primer/probe	Sequence	Ref.
GABRA3 a	GGCAGACATGGCATGATGAA	
GABRA3 b	CTTCAGCTGTTGTATAGGCATAGCTT	
GABRA3 c	CGAGGGCTCAACCTCCAACTT	
GABRA3 d	CATCATGCCATGTCTGCCGAAA	
GABRA3 e	GGAGGCGGAGATTGCACA	
GABRA3 f	GGCATAGCTTCCAAACTTCAGTGGGCAGGCA	
GABRA3 g	GGGGCCATCAAATTTCAGTCTTTCATCATGCCAT	
GABRA3 h	CCTTGACCAGTGGTTCCAGGGAGA	
GABRA3 i	CAACGGTACTACCCTGGGT	
GABRA3 j	CCAAGGCTGGTCATGTAACAGT	
GABRA3 k	ATGAATTCTACTGTTTGCGGATCATGCCCT	
GABRA3 l	GGAGAGACCTGTGACCTTTCT	
GABRA3 m	TGCTGCACTGCCACCACTAT	
GABRA3 u	CGGTCTTCTGACCTCCAATGCGCAA	
GABRA3-probe	FAM-CTGGACACCGGACACCTTCTTCCACAATGGCA-TAMRA	
TET1_F1	CCCGAATCAAGCGGAAGAATA	1
TET1_R1	TACTTCAGGTTGCACGGT	1
ACTINF	CCCTGGACTTCGAGCAAGAGAT	1
ACTINR	AAGGTAGTTTCGTGGATGCCACA	1
TET3_F	GTTCCTGGAGCATGTACTTC	2
TET3_R	CTTCCTCTTTGGGATTGTCC	2
TET1_Xho	ATGACTCGAGAGGCTTTTCTCCCCCTCT	
TET1_NotI	TATGCGGCCGCCCTTGCTTCATGAGAAAGAGCA	
TET3_NotI	TATGCGGCCGCGGGAGGGTAAGGAGGGGTA	
TET3_XhoI	ATGACTCGAGGTGCCAGGGAGCCAGCGT	
TET1_mut1	AAAATAAGCTGAATTATTATTTCATGCAGCCATTGTTCCAACATCTTCCAATC	
TET1_mut2	GAGTATGGAAAACCTAATGCAGCTTCTCCCTTGGAAATGC	
TET1_mut3	CCGCTAACACTTACAATTTTGCAGCAAAAGCAAACAGTTCCAGC	
TET1_mut4	AAACTCATTGTAACTTATTAAAATAATATCTGCAGCAAAGTATCTGTTTTGAGCTTTTGAC	

1. Hsu et al., 2012 *Cell Rep*, 2:568-579
2. Lian et al., 2012 *Cell*, 150:1135-1146